

Improving Infinitely Deep Bayesian Neural Networks with Nesterov’s Accelerated Gradient Method

Chenxu Yu*

Shenzhen Institutes of Advanced Technology
Chinese Academy of Sciences
Shenzhen, P.R.China
yuchenxu1024@163.com

Wenqi Fang†

Shenzhen Institutes of Advanced Technology
Chinese Academy of Sciences
Shenzhen, P.R.China
wq.fang@siat.ac.cn

Abstract—As a representative continuous-depth neural network approach, stochastic differential equation (SDE)-based Bayesian neural networks (BNNs) have attracted considerable attention due to their solid theoretical foundations and strong potential for real-world applications. However, their reliance on numerical SDE solvers inevitably incurs a large number of function evaluations (NFEs), resulting in high computational cost and occasional convergence instability. To address these challenges, we propose a Nesterov-accelerated gradient (NAG) enhanced SDE-BNN model. By integrating NAG into the SDE-BNN framework along with an NFE-dependent residual skip connection, our method accelerates convergence and substantially reduces NFEs during both training and testing. Extensive empirical results show that our model consistently outperforms conventional SDE-BNNs across various tasks, including image classification and sequence modeling, achieving lower NFEs and improved predictive accuracy.

Index Terms—Stochastic differential equation, Bayesian neural network, Nesterov-accelerated gradient, Number of function evaluations

I. INTRODUCTION

Neural networks (NNs) are commonly modeled as discrete sequences of layers, each consisting of an affine transformation followed by a nonlinear activation [1]. This formulation underpins modern deep learning and has driven success across a wide range of applications, including image classification [2], speech recognition [3], and natural language processing [4]. As network depth increases, NNs can be naturally interpreted as discretizations of continuous dynamical systems, providing new perspectives for theoretical analysis, architecture design, and understanding model behavior [5].

As the seminal continuous-depth neural network proposed by Chen et al, Neural Ordinary Differential Equations (Neural ODEs) model hidden states as solutions to an ODE, replacing discrete-layer architectures with continuous-time dynamics [6]. This idea has spawned numerous Neural ODE variants—augmented [7], second-order [8]–[10], control-based [11]–[13], and physically informed [14]–[16]—collectively enhancing the expressivity, efficiency, and

versatility of continuous-depth NNs. These formulations enable Neural ODE-based approaches to excel in time-series forecasting [17], image analysis [18], and dynamical system simulation [19], while providing strong generalization performance and enhanced interpretability.

To account for stochastic noise, Neural SDEs extend Neural ODEs to explicitly model inherent randomness and uncertainty in the data [20]. By embedding NNs in the deterministic drift term, stochastic diffusion term, or both, it offers a flexible framework for modeling complex dynamics that combine structured behavior with randomness, making it well-suited for stochastic process modeling, probabilistic forecasting, and noisy system simulation [21]–[24].

Building upon this idea, the SDE-BNN method incorporates Bayesian uncertainty inference into the Neural SDEs framework, thereby further improving robustness and generalization [25]. Although SDE-BNNs capture uncertainty through parameter distributions, their dependence on iterative SDE solvers leads to excessive function evaluations, increased computational cost, and potentially unstable convergence. To some extent, recent variants, such as partially stochastic SDE-BNN (PSDE-BNN) [26] and rough path theory-based SDE-BNN (RDE-BNN) [27], alleviate these challenges by introducing partial stochasticity into the SDE-BNN architecture.

Unlike prior variants, and inspired by Nesterov-accelerated NODEs [10], we incorporate the Nesterov accelerated gradient (NAG) method into the SDE-BNN framework, termed Nesterov-SDEBNN. The proposed approach improves numerical stability and computational efficiency, thereby accelerating convergence while maintaining—or even enhancing—generalization performance. In contrast to PSDE-BNN and RDE-BNN, which rely on more complex mathematical formulations, Nesterov-SDEBNN achieves these improvements by simply extending the original first-order ODEs in SDE-BNN to second-order dynamics via NAG and revising the residual connection scheme. Experiments on multiple representative open-source datasets show that Nesterov-SDEBNN significantly reduces the NFEs, accelerates convergence, and improves predictive accuracy.

*Work done during the author’s internship at the Shenzhen Institutes of Advanced Technology. †Corresponding author: Wenqi Fang.

The main contributions of this paper are summarized as follows:

- We propose Nesterov-SDEBNN by integrating the NAG method into the original SDE-BNN framework, complemented by an NFE-dependent residual connection strategy to enhance overall performance.
- Compared with the original SDE-BNN, our method converges faster and achieves higher accuracy on image classification and sequence modeling tasks, while significantly reducing NFEs, thereby accelerating both training and testing in adaptive differential equation solvers.

II. RELATED WORK

A. Neural Ordinary Differential Equations

Neural ODEs parameterize continuous-time dynamics using NNs of the form:

$$\frac{dh_t}{dt} = f_\theta(h_t, t), \quad h_0 \in \mathbb{R}^d \quad (1)$$

where h_t denotes the hidden state at time t and $f : \mathbb{R}^d \times \mathbb{R} \rightarrow \mathbb{R}^d$ is a Lipschitz-continuous NN parameterized by θ [6]. The forward pass corresponds to numerically solving this ODE from an initial input state $h_0 = x$, yielding an infinitely deep residual network with universal approximation capability, while enabling memory-efficient training via the adjoint sensitivity method and flexible accuracy–efficiency tradeoffs through adaptive ODE solvers [6]–[10].

B. Nesterov Neural ODEs

To reduce the NFEs and accelerate training and testing, Nguyen et al. [10] introduced the NAG method into Neural ODEs (Nesterov Neural ODE) by extending first-order ODEs to second-order dynamics. Nesterov Neural ODEs were formulated by solving the following second-order differential equation:

$$\frac{d^2 h_t}{dt^2} + \frac{3}{t} \frac{dh_t}{dt} + f_\theta(h_t, t) = 0 \quad (2)$$

To improve computational efficiency and mitigate numerical instability, equation (2) is reformulated as an equivalent first-order system, making it more amenable to NN implementations [10]:

$$\begin{cases} h_t = \sigma_f \left(t^{-\frac{3}{2}} e^{\frac{t}{2}} \right) x_t, \\ x'_t = \sigma_f(m_t), \\ m'_t = -m_t - \sigma_f(f_\theta(h_t, t)) - \xi h_t, \end{cases} \quad (3)$$

Here, x_t denotes an auxiliary variable associated with h_t , m_t represents the momentum term, σ_f is a nonlinear activation function, and ξ controls the residual connection [10]. This reformulation recasts the dynamics as a first-order system that incorporates momentum, leading to accelerated convergence and serving as the basis for our methodology.

C. Stochastic Differential Equations based Bayesian Neural Network

Neural SDEs extend Neural ODEs by introducing stochastic components into the dynamics, enabling the model to capture both deterministic and stochastic behavior [20]:

$$\frac{dh_t}{dt} = f_w(h_t, t) dt + g_\theta(h_t, t) dB_t \quad (4)$$

where f_w and g_θ are the drift and diffusion functions, respectively, and B_t denotes Brownian motion. This formulation allows the network to model randomness inherent in various real-world applications, such as robust pricing and hedging, irregular time series data analysis, and eddy simulation [23], [24], [28].

Building on Neural SDEs, the SDE-BNN framework integrates SDEs with BNNs to capture uncertainty in both system dynamics and network parameters [22], [25]. In this framework, the NN weights are modeled as stochastic processes. Therefore, training SDE-BNNs via variational inference (VI) involves solving an augmented SDE that jointly tracks the trajectories of both the weights and the network activations [25]:

$$d \begin{bmatrix} w_t \\ h_t \end{bmatrix} = \begin{bmatrix} f_\phi(w_t, t) \\ f_{w_t}(h_t, t) \end{bmatrix} dt + \begin{bmatrix} g_\theta(w_t, t) \\ 0 \end{bmatrix} dB_t \quad (5)$$

where f_{w_t} and f_ϕ represent the dynamics of the weights and the activations of the network, respectively. The final hidden unit state h_T ($t \in (0, T]$) is used to parameterize the likelihood of the target output y .

While SDE-BNNs effectively model uncertainty and improve robustness under noisy or incomplete observations, it suffers from a significant drawback: solving SDEs requires huge NFEs, which slows both training and testing. To mitigate this, PSDE-BNN [26] and RDE-BNN [27] introduce partial stochasticity, striking a balance between computational cost and uncertainty modeling. Unlike these methods, our approach tackles this challenge by integrating the NAG method directly into the SDE-BNN framework, offering a simple yet effective solution.

III. METHODOLOGY

In this section, we present details of our Nesterov-SDEBNN approach.

A. Prior Process and Approximate Posterior over Weights

In essence, the proposed Nesterov-SDEBNN adheres to the Bayesian framework and thus admits well-defined prior and posterior distributions.

To obtain a simple prior with bounded marginal variance in the long-time limit, we adopt an Ornstein–Uhlenbeck (OU) process as the prior over the weights, defined by an SDE with the following drift and diffusion terms:

$$f_p(w_t, t) = -w_t, \quad g(w_t, t) = \sigma I_d, \quad (6)$$

where σ is a hyperparameter and I_d is a $d \times d$ identity matrix.

For the posterior, we seek a posterior approximation that can capture non-Gaussian, non-factorized marginals, achieved

by parameterizing its dynamics with a NN whose capacity can be scaled as needed. Accordingly, we implicitly define the approximate posterior over the weights via an SDE with a learned drift:

$$f_q(w_t, t, \phi) = \text{NN}_\phi(w_t, t) - f_p(w_t, t), \quad (7)$$

where the posterior drift, f_q , is parameterized by a small NN with parameters ϕ , while the diffusion terms are kept the same as the prior.

B. Evaluation of the Network

By incorporating the NAG method into the SDE-BNN framework, we can easily derive the modified dynamics by combining equations (3) and (5), expressed in terms of the joint state $H_t := (x_t, m_t, w_t)$:

$$h_t = \sigma_f \left(t^{-\frac{3}{2}} e^{\frac{t}{2}} \right) x_t, \\ dH_t = \begin{bmatrix} \sigma_f(m_t) \\ -m_t - \sigma_f(f_{w_t}(h_t, t)) - \xi h_t \\ f_\phi(w_t, t) \end{bmatrix} dt + \begin{bmatrix} 0 \\ 0 \\ g(w_t, t) \end{bmatrix} dB_t. \quad (8)$$

Notably, the residual term ξh_t in equation (8) is added to evaluate the drift of m_t . Due to the time-stepping nature of SDE solvers, each increment of NFE_f (denotes the number of drift function evaluations) advances the joint state from H_t to $H_{t+\Delta t}$. Specifically, to evolve the state from m_t to $m_{t+\Delta t}$, the feature h_t is first processed by the function f_{w_t} with weight w_t and activation σ_f , and then combined with the residual ξh_t and the current state m_t . After solving equation (8), we obtain $h_{t+\Delta t}$ and $m_{t+\Delta t}$. These processes are repeated iteratively until the final time T , as illustrated in subfigure (a) of Figure 1. Therefore, this residual mechanism establishes explicit link between representation at successive time steps (e.g., $m_t \rightarrow m_{t+\Delta t} \rightarrow m_{t+2\Delta t}$) rather than within a single time step. However, these settings result only in a direct residual connection, rather than the residual skip connection defined in the original formulation [29]. This discrepancy may reduce feature reuse and constrain the effectiveness of residual learning in the SDEBNN settings.

To better align with classic residual learning, rather than injecting residual at every drift evaluation, we propose an NFE_f -dependent residual skip connection mechanism. Specifically, we modify the drift of m_t as:

$$\frac{dm_t}{dt} = -m_t - \sigma_f(f_{w_t}(h_t, t) + \epsilon \xi h_{\text{temp}}), \quad (9)$$

where the control variables ϵ and h_{temp} (initialized as input x , and retained from the previous value when NFE_f is odd) depend on NFE_f , defined as:

$$\epsilon = \begin{cases} 1, & \text{if } \text{NFE}_f \text{ is odd} \\ 0, & \text{if } \text{NFE}_f \text{ is even} \end{cases}, h_{\text{temp}} = h_t \text{ if } \text{NFE}_f \text{ is even.} \quad (10)$$

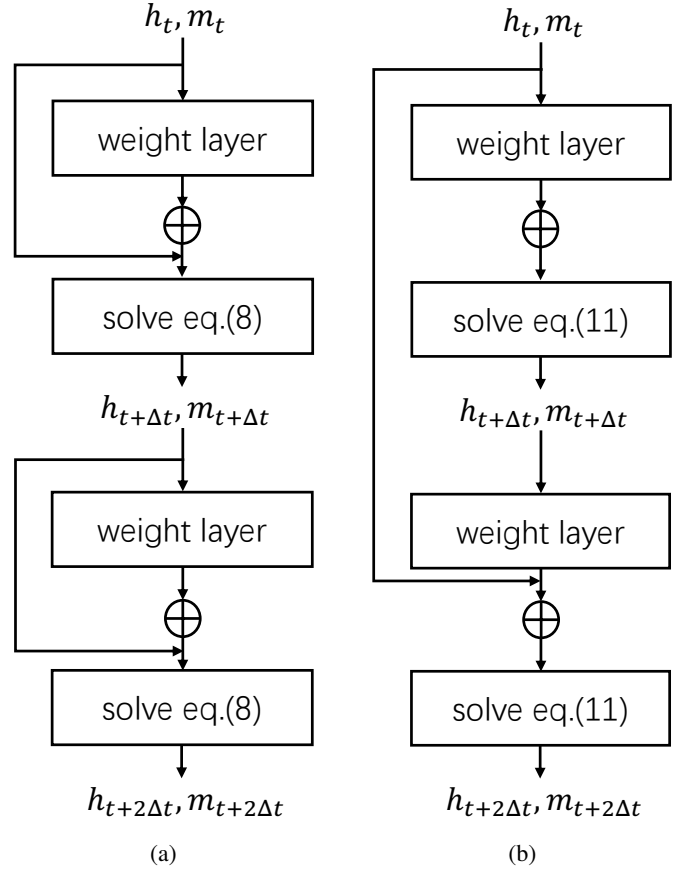


Fig. 1: Comparison of mentioned residual mechanisms: (a) Direct residual connection for m_t in eq (8). (b) Proposed NFE_f -dependent residual skip connection for m_t in eq (11).

Consequently, the final formulation of our Nesterov-SDEBNN method becomes:

$$h_t = \sigma_f \left(t^{-\frac{3}{2}} e^{\frac{t}{2}} \right) x_t, \\ dH_t = \begin{bmatrix} \sigma_f(m_t) \\ -m_t - \sigma_f(f_{w_t}(h_t, t) + \epsilon \xi h_{\text{temp}}) \\ f_\phi(w_t, t) \end{bmatrix} dt + \begin{bmatrix} 0 \\ 0 \\ g(w_t, t) \end{bmatrix} dB_t. \quad (11)$$

As described in equations (9) and (10), the proposed NFE_f -dependent scheme adheres to the spirit of residual skip connections, as shown in subfigure (b) of Figure 1. When NFE_f is odd, the feature h_t is cached for use at time $t + \Delta t$; when NFE_f becomes even ($\neq 0$), the cached feature is injected into the drift at $t + \Delta t$ to help produce $m_{t+2\Delta t}$. This mechanism creates a skip connection across two consecutive drift evaluations, reusing cached representations to improve information flow without adding parameters. Meanwhile, this formulation allows the state $m_{t+2\Delta t}$ to depend explicitly on both h_t and $h_{t+\Delta t}$, rather than only on $h_{t+\Delta t}$ as in equation (8), which may help mitigate vanishing gradient issues commonly encountered in SDE solvers.

To compute h_t given $x_0 = h_0 = x$, we marginalize over weight trajectories via Monte Carlo sampling. Specifically, we

sample paths $\{w_t\}$ from the posterior process, and for each path solve equation (11) to obtain $\{h_t\}$. The learnable parameters include the initial weights w_0 and the drift parameters ϕ .

C. Output Likelihood

Predictions are generated from the final hidden representation h_T , which directly parameterizes the output likelihood: $\log p(y|x, w) = \log p(y|h_T)$. In practice, this likelihood can be chosen as a Gaussian distribution for regression tasks or a categorical distribution for classification.

D. Training objective

To train our Nesterov-SDEBNN model, we adopt the VI framework, in which the loss function is derived from the evidence lower bound (ELBO) by Monte Carlo sampling [25], defined as:

$$\mathcal{L}_{\text{ELBO}}(\phi) = \mathbb{E}_{q_\phi(w)} \left[\log p(y|x, w) - \int_0^T \frac{1}{2} \|u(w_t, t, \phi)\|_2^2 dt \right] \quad (12)$$

where $u(w_t, t, \phi) = g(w_t, t)^{-1} [f_q(w_t, t, \phi) - f_p(w_t, t)]$, $q_\phi(w)$ denotes the posterior distribution of w for short. The sampled weights, hidden activations, and training objective can be computed simultaneously via a single SDE solver call [25].

IV. EXPERIMENTS

In this section, we empirically evaluate the proposed Nesterov-SDEBNN against the baseline SDE-BNN on a diverse set of benchmark tasks, including toy regression, image classification, and dynamical simulation. These benchmarks cover multiple data modalities, ranging from images to time-series data. All experiments were implemented using PyTorch and conducted on a remote server equipped with an NVIDIA A100 GPU (40 GB memory) and an Intel Xeon Gold 5320 CPU (26 cores). Additional details on training procedures, model configurations, and datasets are provided in Table I. The block configurations follow those of the original SDE-BNN approach [25].

A. Toy 1D Regression

We first validate the capabilities of Nesterov-SDEBNN on a simple 1D regression problem. To model non-monotonic functions, we augment the state space by adding two additional dimensions initialized to zero. As shown in Figure 2, our model retains the expressive posterior predictive power of SDE-BNN on synthetic non-monotonic noisy 1D data, demonstrating its effectiveness on this simple fitting task.

B. Image Classification

For image classification, we followed the SDE-BNN setup, using convolutional networks to model instantaneous hidden-state changes. We benchmarked Nesterov-SDEBNN against SDE-BNN on MNIST and CIFAR-10 in terms of accuracy, negative log-likelihood (NLL), area under the curve (AUC), and NFEs, with results reported in Table II, Figures 3 and 4.

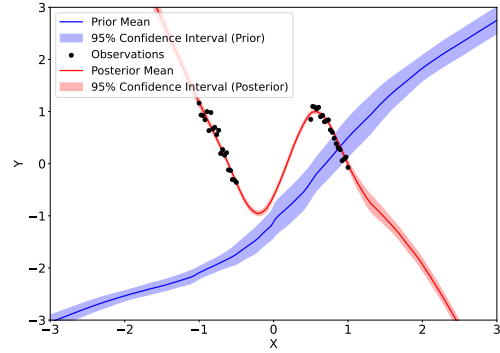


Fig. 2: Predictive prior and posterior of Nesterov-SDEBNN on a non-monotonic toy dataset. The blue and red shaded regions denote the 95% confidence intervals of the prior and posterior, respectively, while the solid lines represent their corresponding mean predictions.

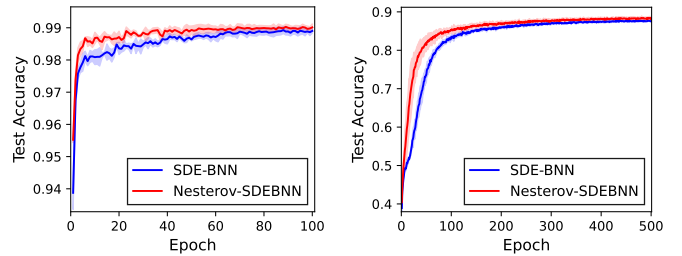


Fig. 3: Comparison of test accuracy between SDE-BNN and Nesterov-SDEBNN: (Left) MNIST (Right) CIFAR-10.

Table II summarizes the performance of SDE-BNN and Nesterov-SDEBNN on MNIST and CIFAR-10 datasets under both fixed-step and adaptive integration schemes. Across all settings, Nesterov-SDEBNN consistently achieves slightly higher accuracy and AUC than the standard SDE-BNN. Notably, the NLL values are significantly lower for Nesterov-SDEBNN, indicating improved predictive uncertainty. On MNIST, the fixed-step Nesterov-SDEBNN reaches 99.04% accuracy and 7.37×10^{-2} NLL, compared to 98.90% and 14.37×10^{-2} for SDE-BNN. On CIFAR-10, similar trends are observed, with Nesterov-SDEBNN improving both accuracy (88.36% vs. 87.60%), AUC (85.61% vs. 83.05%), and NLL (5.97×10^{-1} vs. 9.89×10^{-1}) under fixed-step conditions. In addition, in adaptive integration scenarios, Nesterov-SDEBNN consistently reduces NLL while simultaneously improving predictive accuracy. This dual improvement underscores the model's robustness in both discriminative performance and uncertainty calibration, regardless of the underlying step-size scheme or dataset complexity.

Figure 3 compares the test accuracy of the two models. While both achieve similar final accuracy, the Nesterov-SDEBNN curve consistently lies above that of SDE-BNN throughout testing, resulting in a larger AUC value. This indicates that Nesterov-SDEBNN converges faster and achieves higher accuracy in the early stages of training on both the

TABLE I: The following hyperparameters are used for each evaluation method corresponding to the experimental results reported in the paper.

Model	Hyper-parameter	Experiments			
		1D Regression	MNIST [30]	CIFAR-10 [31]	Walker2D [32]
SDE-BNN (fixed step)					
and Nesterov-SDE-BNN (fixed step)					
	Augment dim.	2	2	2	0
	# blocks	1	1	1-1-1	1
	Diffusion σ	0.2	0.1	0.1	0.1
	KL coef.	0.0	1e-5	100	1
	Learning Rate	1e-3	1e-3	3e-4	{0:1e-3, 50:3e-3}
	# Solver Steps	20	20	50	50
	Batch Size	50	128	128	256
	Activation	swish	swish	mish	tanh
	Epochs	1000	100	500	500
	Drift f_x dim.	32	32	64	24
	Drift f_w dim.	32	1-64-1	2-32-2	1-32-1
	# Posterior Samples	10	1	1	1
	solver	midpoint	midpoint	midpoint	midpoint
SDE-BNN (adaptive)					
and Nesterov-SDE-BNN (adaptive)					
	<SDE-BNN>	-	<SDE-BNN>	<SDE-BNN>	<SDE-BNN>
	atol	-	1e-3	5e-3	5e-3
	rtol	-	1e-3	5e-3	5e-3
	Epochs	-	100	300	500
	Activation	-	swish	swish	tanh
	solver	midpoint	midpoint	midpoint	midpoint

TABLE II: Quantitative evaluation on MNIST and CIFAR-10. Comparison of SDE-BNN and Nesterov-SDEBNN performance (Accuracy, AUC, and NLL) using fixed-step and adaptive-step integration.

Model	MNIST			CIFAR-10		
	Accuracy (%) \uparrow	AUC (%) \uparrow	NLL ($\times 10^{-2}$) \downarrow	Accuracy (%) \uparrow	AUC (%) \uparrow	NLL ($\times 10^{-1}$) \downarrow
SDE-BNN(fixed step)	98.90 \pm 0.07	97.59 \pm 0.04	14.37 \pm 0.89	87.56 \pm 0.36	83.05 \pm 0.29	9.89 \pm 0.22
Nesterov-SDEBNN(fixed step)	99.04 \pm 0.12	97.87 \pm 0.06	7.37 \pm 0.65	88.36 \pm 0.24	85.61 \pm 0.45	5.97 \pm 0.11
SDE-BNN(adaptive step)	98.87 \pm 0.12	97.57 \pm 0.03	13.85 \pm 1.26	85.87 \pm 0.28	78.42 \pm 0.60	6.77 \pm 0.09
Nesterov-SDEBNN(adaptive step)	99.04 \pm 0.03	97.88 \pm 0.04	7.15 \pm 0.34	86.99 \pm 0.23	83.94 \pm 0.32	5.32 \pm 0.10

MNIST and CIFAR-10 datasets.

Furthermore, we compares the test NFEs between SDE-BNN and Nesterov-SDEBNN on MNIST and CIFAR-10, as shown in Figure 4. On both datasets, Nesterov-SDEBNN consistently requires significantly fewer NFEs than SDE-BNN throughout training, indicating more efficient computation. For MNIST, SDE-BNN’s NFE increases steadily and fluctuates around 400, whereas Nesterov-SDEBNN remains stable near 240. On CIFAR-10, SDE-BNN’s NFE rises sharply after around 50 epochs and plateaus near 270, while Nesterov-SDEBNN stabilizes around 170, demonstrating faster convergence and lower computational cost compared to SDE-BNN.

These results demonstrate that Nesterov-SDEBNN delivers superior classification performance while significantly reducing computational overhead, making it a highly efficient solution for image classification.

C. Walker2D Kinematic Simulation

To evaluate the model’s capacity for capturing long-term dependencies [33], we applied Nesterov-SDEBNN to Walker2D kinematic simulation data [32]. Building on the ODE-RNN framework [34], we benchmarked our approach against the standard SDE-BNN.

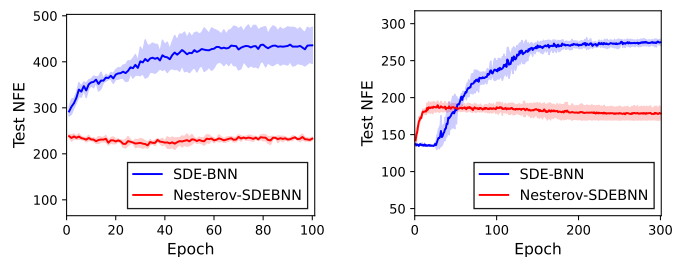


Fig. 4: Comparison of test NFEs between SDE-BNN and Nesterov-SDEBNN: (Left) MNIST (Right) CIFAR-10.

As shown in Figure 5, Nesterov-SDEBNN reduces loss faster and achieves lower final error rates than standard counterparts. Despite slightly higher volatility and oscillations during testing, it maintains superior performance throughout the 500 epochs, with its mean loss curve generally below the baseline.

Furthermore, as illustrated in Figure 6, Nesterov-SDEBNN demonstrates superior efficiency during both training and testing phases. While it initially incurs slightly higher NFEs, it quickly stabilizes around 145, maintaining a consistent compu-

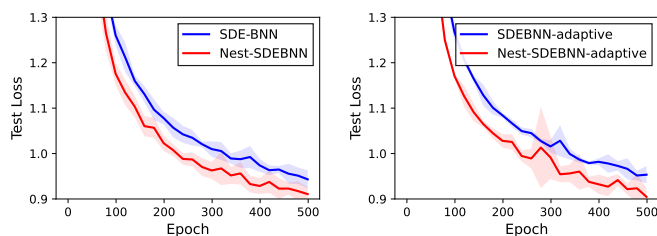


Fig. 5: Walker2D test loss performance. Nesterov-SDEBNN vs. SDE-BNN under fixed-step (Left) and adaptive-step (Right) solver configurations.

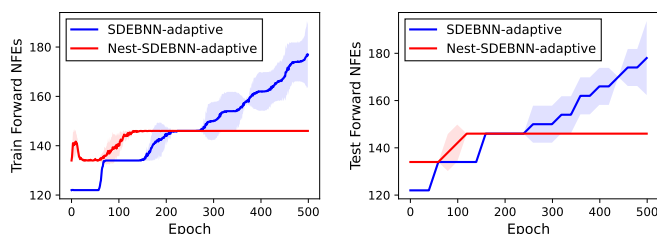


Fig. 6: Forward-pass NFEs on the Walker2D kinematic simulation. Comparison between SDE-BNN and Nesterov-SDEBNN during (Left) training and (Right) testing using adaptive-step solver.

tational cost. In contrast, standard SDE-BNN shows a stepwise increase in complexity, reaching 180 NFEs, about 24% higher than ours. These results indicate that integrating Nesterov-like dynamics into the SDE-BNN framework effectively limits solver complexity, resulting in more predictable and efficient inference than the standard adaptive approach.

Overall, these results provide further compelling empirical evidence that our approach outperforms the SDE-BNN baseline, underscoring its effectiveness and practical potential for time-series modeling.

V. CONCLUSION

In this paper, we introduced Nesterov-SDEBNN, an advancement of the SDE-BNN framework that integrates Nesterov accelerated gradient principles with an NFE-dependent residual scheme. This architecture significantly curtails the computational overhead of training and testing by reducing the required number of function evaluations. Empirical results show that our approach converges faster and achieves higher accuracy on various tasks such as image classification and time-series modeling, indicating its stronger capacity to capture complex patterns than standard SDE-BNNs. Our future work will assess the framework’s scalability and robustness on larger, more complex datasets and explore extensions to examine its potential in practical applications.

ACKNOWLEDGMENTS

W.Fang was supported by the National Natural Science Foundation of China (NSFC) under Grant No.12401676.

REFERENCES

- [1] Paulo Botelho Pires, José Duarte Santos, and Inês Veiga Pereira. Artificial neural networks: history and state of the art. *Encyclopedia of Information Science and Technology, Sixth Edition*, pages 1–25, 2025.
- [2] Yaoli Wang, Yaojun Deng, Yuanjin Zheng, Pratik Chattopadhyay, and Lipo Wang. Vision transformers for image classification: A comparative survey. *Technologies*, 13(1):32, 2025.
- [3] Harsh Ahlawat, Naveen Aggarwal, and Deepti Gupta. Automatic speech recognition: A survey of deep learning techniques and approaches. *International Journal of Cognitive Computing in Engineering*, 2025.
- [4] Farid Ariai, Joel Mackenzie, and Gianluca Demartini. Natural language processing for the legal domain: A survey of tasks, datasets, models, and challenges. *ACM Computing Surveys*, 58(6):1–37, 2025.
- [5] Chao Ma, Lei Wu, et al. Machine learning from a continuous viewpoint, i. *Science China Mathematics*, 63(11):2233–2266, 2020.
- [6] Ricky T. Q. Chen, Yulia Rubanova, Jesse Bettencourt, and David Duvenaud. Neural ordinary differential equations. *Advances in Neural Information Processing Systems*, 2018.
- [7] Emilien Dupont, Arnaud Doucet, and Yee Whye Teh. Augmented neural odes. *Advances in neural information processing systems*, 32, 2019.
- [8] Alexander Norcliffe, Cristian Bodnar, Ben Day, Nikola Simidjievski, and Pietro Liò. On second order behaviour in augmented neural odes. *Advances in neural information processing systems*, 33:5911–5921, 2020.
- [9] Cagatay Yildiz, Markus Heinonen, and Harri Lahdesmaki. Ode2vae: Deep generative second order odes with bayesian neural networks. *Advances in Neural Information Processing Systems*, 32, 2019.
- [10] Ho Huu Nghia Nguyen, Tan Nguyen, Huyen Vo, Stanley Osher, and Thieu Vo. Improving neural ordinary differential equations with nesterov’s accelerated gradient method. *Advances in Neural Information Processing Systems*, 35:7712–7726, 2022.
- [11] Patrick Kidger, James Morrill, James Foster, and Terry Lyons. Neural controlled differential equations for irregular time series. *Advances in neural information processing systems*, 33:6696–6707, 2020.
- [12] Thomas Asikis, Lucas Böttcher, and Nino Antulov-Fantulin. Neural ordinary differential equation control of dynamics on graphs. *Physical Review Research*, 4(1):013221, 2022.
- [13] Pengkai Wang, Song Chen, Jiayu Liu, Shengze Cai, and Chao Xu. Pidnodes: Neural ordinary differential equations inspired by a proportional–integral–derivative controller. *Neurocomputing*, 614:128769, 2025.
- [14] Samuel Greydanus, Misko Dzamba, and Jason Yosinski. Hamiltonian neural networks. *Advances in neural information processing systems*, 32, 2019.
- [15] Miles Cranmer, Sam Greydanus, Stephan Hoyer, Peter Battaglia, David Spergel, and Shirley Ho. Lagrangian neural networks. *arXiv preprint arXiv:2003.04630*, 2020.
- [16] Marc Finzi, Ke Alexander Wang, and Andrew G Wilson. Simplifying hamiltonian and lagrangian neural networks via explicit constraints. *Advances in neural information processing systems*, 33:13880–13889, 2020.
- [17] Yongkyung Oh, Seungsu Kam, Jonghun Lee, Dong-Young Lim, Sungil Kim, and Alex Bui. Comprehensive review of neural differential equations for time series analysis. *arXiv preprint arXiv:2502.09885*, 2025.
- [18] Hao Niu, Yuxiang Zhou, Xiaohao Yan, Jun Wu, Yuncheng Shen, Zhang Yi, and Junjie Hu. On the applications of neural ordinary differential equations in medical image analysis. *Artificial Intelligence Review*, 57(9):236, 2024.
- [19] Ashish S Nair, Shivam Barwey, Pinaki Pal, Jonathan F MacArt, Troy Arcomano, and Romit Maulik. Understanding latent timescales in neural ordinary differential equation models of advection-dominated dynamical systems. *Physica D: Nonlinear Phenomena*, 476:134650, 2025.
- [20] Xuanqing Liu, Tesi Xiao, Si Si, Qin Cao, Sanjiv Kumar, and Cho-Jui Hsieh. Neural sde: Stabilizing neural ode networks with stochastic noise. *arXiv preprint arXiv:1906.02355*, 2019.
- [21] Junteng Jia and Austin R Benson. Neural jump stochastic differential equations. *Advances in Neural Information Processing Systems*, 32, 2019.
- [22] Xuechen Li, Ting-Kam Leonard Wong, Ricky TQ Chen, and David Duvenaud. Scalable gradients for stochastic differential equations. In *International Conference on Artificial Intelligence and Statistics*, pages 3870–3882. PMLR, 2020.

- [23] Anudhyan Boral, Zhong Yi Wan, Leonardo Zepeda-Núñez, James Lottes, Qing Wang, Yi-fan Chen, John Anderson, and Fei Sha. Neural ideal large eddy simulation: Modeling turbulence with neural stochastic differential equations. *Advances in neural information processing systems*, 36:69270–69283, 2023.
- [24] YongKyung Oh, Dong-Young Lim, and Sungil Kim. Stable neural stochastic differential equations in analyzing irregular time series data. *arXiv preprint arXiv:2402.14989*, 2024.
- [25] Winnie Xu, Ricky TQ Chen, Xuechen Li, and David Duvenaud. Infinitely deep bayesian neural networks with stochastic differential equations. In *International Conference on Artificial Intelligence and Statistics*, pages 721–738. PMLR, 2022.
- [26] Sergio Calvo-Ordonez, Matthieu Meunier, Francesco Piatti, and Yuantao Shi. Partially stochastic infinitely deep bayesian neural networks. *arXiv preprint arXiv:2402.03495*, 2024.
- [27] YANG Xiaoyu, QIU Peiyi, et al. Infinitely deep bayesian neural network with signature transform. *Neurocomputing*, page 132563, 2025.
- [28] Patryk Gierjatorowicz, Marc Sabate Vidales, David Siska, Lukasz Szpruch, and Zan Zuric. Robust pricing and hedging via neural stochastic differential equations. *Journal of Computational Finance*, 26(3):1–32, 2022.
- [29] Kaiming He, Xiangyu Zhang, Shaoqing Ren, and Jian Sun. Deep residual learning for image recognition. In *Proceedings of the IEEE conference on computer vision and pattern recognition*, pages 770–778, 2016.
- [30] Li Deng. The mnist database of handwritten digit images for machine learning research. *IEEE Signal Processing Magazine*, 29(6):141–142, 2012.
- [31] Alex Krizhevsky, Vinod Nair, and Geoffrey Hinton. The cifar-10 dataset. *online: <http://www.cs.toronto.edu/kriz/cifar.html>*, 55:5, 2014.
- [32] Emanuel Todorov, Tom Erez, and Yuval Tassa MuJoCo. A physics engine for model-based control. In *Proceedings of the 2012 IEEE/RSJ International Conference on Intelligent Robots and Systems*, pages 5026–5033.
- [33] M Lechner and R Hasani. Learning long-term dependencies in irregularly-sampled time series. arxiv 2020. *arXiv preprint arXiv:2006.04418*.
- [34] Yulia Rubanova, Ricky TQ Chen, and David K Duvenaud. Latent ordinary differential equations for irregularly-sampled time series. *Advances in neural information processing systems*, 32, 2019.